THE ROYAL SOCIETY

Received 5 July 2001
Accepted 9 October 2001
Published online 1 February 2002

Generation of periodic waves by landscape features in cyclic predator–prey systems

J. A. Sherratt[1], X. Lambin[2], C. J. Thomas[3] and T. N. Sherratt[3*]

[1]*Department of Mathematics, Heriot-Watt University, Edinburgh EH14 4AS, UK*
[2]*Department of Zoology, University of Aberdeen, Tillydrone Avenue, Aberdeen AB24 2TZ, UK*
[3]*Department of Biological Sciences, University of Durham, South Road, Durham DH1 3LE, UK*

The vast majority of models for spatial dynamics of natural populations assume a homogeneous physical environment. However, in practice, dispersing organisms may encounter landscape features that significantly inhibit their movement. We use mathematical modelling to investigate the effect of such landscape features on cyclic predator–prey populations. We show that when appropriate boundary conditions are applied at the edge of the obstacle, a pattern of periodic travelling waves develops, moving out and away from the obstacle. Depending on the assumptions of the model, these waves can take the form of roughly circular 'target patterns' or spirals. This is, to our knowledge, a new mechanism for periodic-wave generation in ecological systems and our results suggest that it may apply quite generally not only to cyclic predator–prey interactions, but also to populations that oscillate for other reasons. In particular, we suggest that it may provide an explanation for the observed pattern of travelling waves in the densities of field voles (*Microtus agrestis*) in Kielder Forest (Scotland–England border) and of red grouse (*Lagopus lagopus scoticus*) on Kerloch Moor (northeast Scotland), which in both cases move orthogonally to any large-scale obstacles to movement. Moreover, given that such obstacles to movement are the rule rather than the exception in real-world environments, our results suggest that complex spatio-temporal patterns such as periodic travelling waves are likely to be much more common in the natural world than has previously been assumed.

Keywords: travelling wave; obstacle; reaction–diffusion; cyclic dynamics; field vole

1. INTRODUCTION

The vast majority of models for spatio-temporal dynamics of natural populations have assumed that populations are distributed in homogeneous environments. In particular, minimal attention has been given to the role of large-scale landscape features that will significantly inhibit the movement of dispersing organisms. Broadly speaking, such organisms can either find a route around such landscape features, refrain from moving altogether or simply attempt to traverse the obstacle. In this paper, we investigate for the first time, to our knowledge, the effects of these simple movement rules on the predicted overall spatio-temporal dynamics of cyclic predator–prey systems.

We begin our investigation using a reaction–diffusion-type model. This assumes that both predator and prey populations move continuously in space; and in the following we will discuss an alternative model that instead assumes that individuals occupy discrete but interconnected spatial sites. Throughout, we study predator–prey systems that are cyclic, meaning that in the absence of any spatial variation both prey and predator densities oscillate. Our model equations, detailed in Appendix A, are a standard model for this type of predator–prey system and we solve them on a two-dimensional domain with no-flux boundary conditions, meaning that individuals cannot enter or leave the domain. When the domain is homogeneous, randomly generated initial population densities rapidly even out, giving spatially uniform population cycles.

Our objective is to consider how large landscape features affect dynamical behaviour. To this end, we introduced into the domain a central obstacle, assuming either no-flux boundary conditions on the edge of the obstacle or that the population densities are always zero on the obstacle edge. The latter would correspond to individuals attempting to cross the obstacle, but always dying in the attempt. With no-flux boundary conditions, the obstacle has little effect on the population dynamics that quickly form uniform oscillations. However, when the population densities are zero around the obstacle, the behaviour is quite different (figure 1*a*; movie clips corresponding to this and other figures are available at http://www.ma.hw.ac.uk/~jas/supplements/obstacles/). The randomness of the initial conditions rapidly disappears, giving rise to periodic travelling waves moving out from the obstacle and through the domain. In these waves, there are again population cycles; however, the cycles are out of phase at different points in space and it is this that constitutes the travelling waves.

Spatio-temporal patterns resembling periodic travelling waves have been observed recently in several natural populations, including field voles (*Microtus agrestis*) (Lambin *et al.* 1998; MacKinnon *et al.* 2001) and red grouse (*Lagopus lagopus scoticus*) (Moss *et al.* 2000). In both of these cases, the underlying cause of these waves remains unknown. Previous modelling work has also shown that periodic waves are generated by invasions in cyclic populations (Sherratt *et al.* 1997, 2000), but there is no evidence for such an invasion in these two cases. We will show that the generation of periodic waves by

*Author for correspondence (t.n.sherratt@durham.ac.uk).

obstacles, in a manner broadly similar to figure 1*a*, is a robust mechanism that provides a possible explanation for the observed behaviour in both field voles and red grouse.

2. DETAILED INVESTIGATION OF THE TRAVELLING WAVES

We have varied extensively both model parameters and the form of the obstacle, and the generation of periodic waves is a consistent feature of our simulations. For example, figure 1*b* shows periodic waves generated by each of three separate obstacles within the domain. The three sets of waves interact and those produced by the largest of the obstacles dominates the overall behaviour. Note that the parameter values used in figure 1*a*,*b* are based on estimates for the field vole–weasel prey–predator interaction; the basis for these parameters is discussed briefly at the end of Appendix A. The domain in the figures is then *ca.* 100 km^2 and the travelling wave moves at *ca.* 3 km yr^{-1}. This is significantly less than the speed observed in the data (15–20 km yr^{-1} (Lambin *et al.* 1998; MacKinnon *et al.* 2001)), but within the levels of uncertainty arising from poor data on dispersal rates.

In our various simulations, we have only seen one qualitatively different type of behaviour. When the ratio of prey to predator birth rates is relatively small (close to 1), or when the consumption of prey by predators saturates at low prey densities, periodic waves are visible close to the obstacle, but decay into irregular oscillations further away (figure 1*c*). In order to explain this second type of behaviour and to better understand the phenomenon overall, we performed a detailed numerical study in one space dimension. Barrier shape is clearly not an issue in one dimension and we consider simply a domain with no-flux conditions at one end and zero population density at the other; this corresponds to the region between the edge of the domain and the obstacle. Again, random initial conditions rapidly develop into periodic travelling waves, moving away from the 'obstacle' (figure 2*a*). By gradually changing parameters towards those for which irregular oscillations are seen in two dimensions, we found that the irregularities arise because the periodic wave generated by the obstacle is an unstable solution. Thus it is seen close to the obstacle, but decays rapidly as it propagates.

An oscillatory system of the type we are considering has a whole family of periodic-wave solutions, with different speeds and amplitudes. The slowest waves have low amplitude and short wavelength, while the fast waves have high amplitude and long wavelength (see Murray (1989) for a review). This wave family is a function of the model and parameters only, independent of the domain and of the boundary and initial conditions. Therefore, in solutions such as those illustrated in figures 1 and 2*a*, a landscape feature is selecting a particular member of the wave family and it is natural to ask whether this selection (and thus the wave speed and amplitude) depends on the (random) initial conditions. We have answered this using one-dimensional simulations. With a fixed set of parameters, we calculated the solution from a range of different initial conditions, obtaining in each case a plot of the solution against space at a given time. We then superimposed these plots, applying an appropriate translation so that the oscillations are in phase. This shows clearly (figure 2*b*) that the periodic wave is the same in all cases, independent of initial conditions—the differences near the two boundaries reflect the different initial conditions. This is an important indicator of the robustness of our mechanism of periodic-wave generation.

A second important issue for robustness is whether the periodic waves depend strictly on our assumption of zero population densities of both predators and prey at the edges of the obstacle. We investigated this further, again in one space dimension, by allowing the predator population to move through the obstacle, with the prey density zero; this could correspond, for example, to a river or lake acting as an obstacle for terrestrial prey, but not for an avian predator. Again, our simulations show periodic waves moving away from the obstacle (not shown for brevity). The predator dispersal within the landscape feature does alter the periodic-wave speed and amplitude, but only slightly. A more significant effect is that there is an appreciably longer transient behaviour, consisting of small bands of waves moving in different directions. However, the long-term behaviour remains the same with travelling waves moving out from the obstacle.

3. COUPLED MAP LATTICE MODEL

Many natural populations do not exist in continuous spatial environments, but rather are restricted to discrete, interconnected patches. In such cases, a coupled map lattice model is a better representation of the population than the reaction–diffusion model that we have been using. Models of this kind have recently been used by Sherratt *et al.* (2000) to study the form of travelling waves in field vole populations, although landscape features were not included in this work. We consider a coupled map lattice model on a square grid of patches, based on the formulation used by Hassell *et al.* (1991). Each generation is divided into two substeps. In the first substep, the predator and prey densities in each patch evolve according to a standard discrete-time predator–prey model, and in the second substep, we assume that a given proportion of the populations move to each of the neighbouring four patches. This is a standard discrete representation of local dispersal; details of the model are given in Appendix B.

In comparison with the reaction–diffusion model discussed above, the behaviour in the coupled map lattice model is somewhat more complex because there is a range of possible behaviours even without landscape features. When predator and prey motility is high, random initial conditions do develop into spatially uniform oscillations on a homogeneous domain, as for the reaction–diffusion model (figure 3*a*). However, for lower and more realistic motility parameters, the long-term solution has the form of one or more spiral waves (figure 3*b*,*c*); a case with many interacting spirals, such as figure 3*c*, has a highly irregular appearance when viewed as a movie (available at http://www.ma.hw.ac.uk/~jas/ supplements/obstacles/).

In this coupled map lattice model, our landscape feature consists of a group of whole patches. Our movement rule implies that in a patch immediately adjacent to this obstacle, a proportion of the population will enter the obstacle at each generation and a 'boundary condition' corresponds to a rule for the fate of these individuals. We have studied three such rules:

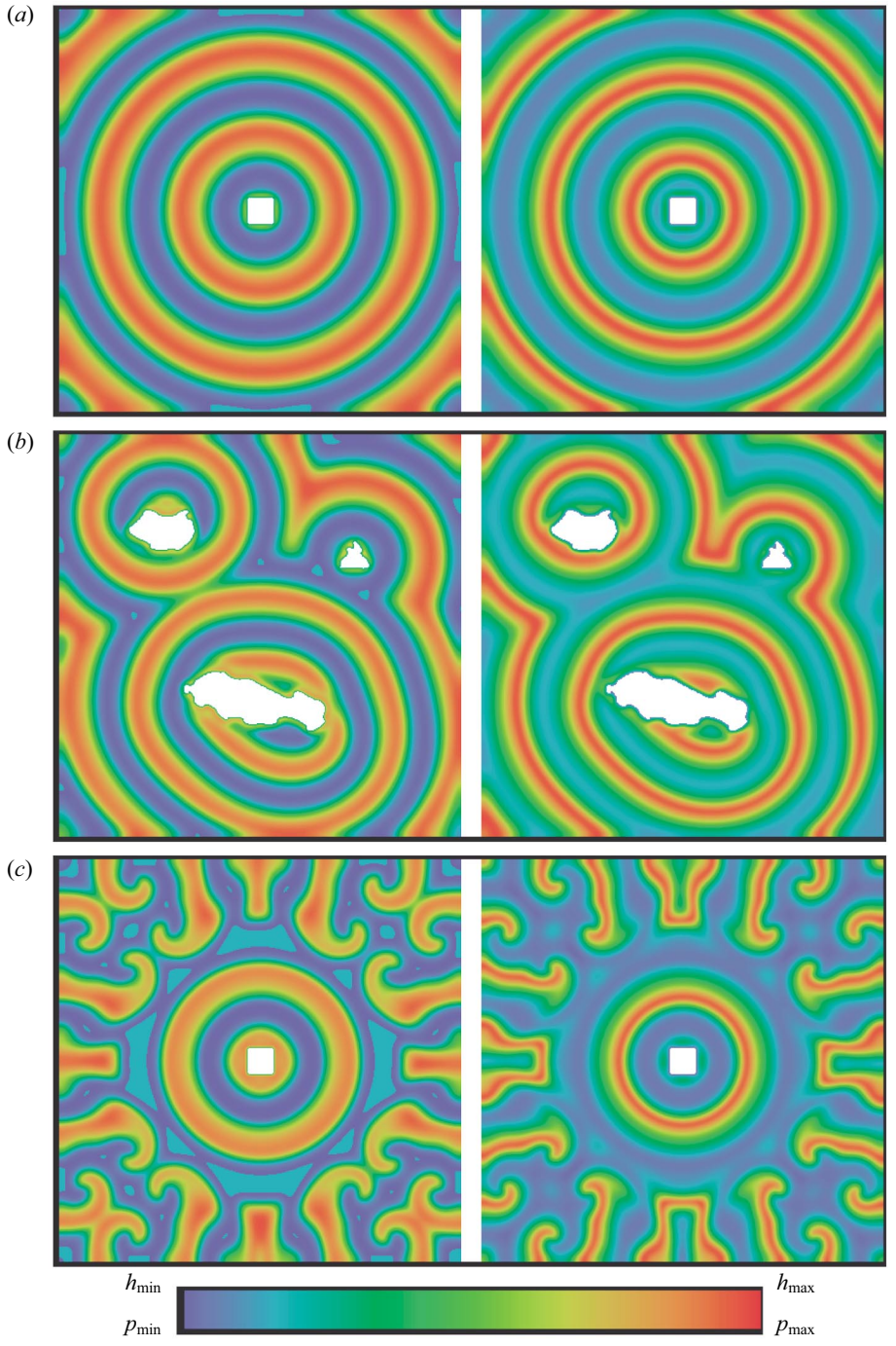

Figure 1. Solutions of the reaction–diffusion model. We plot the prey and predator densities in space at a single time-point. (*a*) Generation of periodic travelling waves from a single, central obstacle. (*b*) Generation of periodic travelling waves from three separate obstacles. Each obstacle generates waves, but those from the largest obstacle dominate the solution. (*c*) Oscillations that are irregular, but retain some aspects of the periodic-wave character; these occur because the selected periodic wave is unstable. In each case, the boundary conditions are zero predator and prey densities at edge of the obstacle and zero flux at the edge of the domain. The domain is a square with side-length of 400 dimensionless space units and the solution is plotted at a dimensionless time of 1000. The model equations (A 2) are detailed in Appendix A. The dimensionless parameter values are: $A = 1.8$, $B = 1.2$, $\delta = 2.0$ and (*a*,*b*) $C = 4.9$; (*c*) $C = 6.0$. The scale bar uses a linear scale and the limits are chosen differently in each part for maximum clarity: (*a*) $h_{min} = 0.03$, $h_{max} = 0.85$, $p_{min} = 0.05$, $p_{max} = 0.6$; (*b*) $h_{min} = 0.03$, $h_{max} = 0.84$, $p_{min} = 0.007$, $p_{max} = 0.6$; (*c*) $h_{min} = 0.005$, $h_{max} = 0.93$, $p_{min} = 0.02$, $p_{max} = 0.61$. The equations are solved numerically using an alternating-direction implicit Crank–Nicolson method. Movie clips corresponding to each part of this figure are available at http://www.ma.hw.ac.uk/~jas/supplements/obstacles/.

(i) the individuals that would enter the obstacle all die;
(ii) they 'deflect' from the obstacle and move to one of the other adjacent patches; and
(iii) they 'stay put', remaining on the patch at the boundary of the obstacle.

Note that the 'die' rule corresponds to the zero population boundary conditions in the reaction–diffusion model and the 'stay put' rule corresponds to a no-flux condition; the 'deflect' rule has no reaction–diffusion analogue.

As one might expect from the results of the reaction–

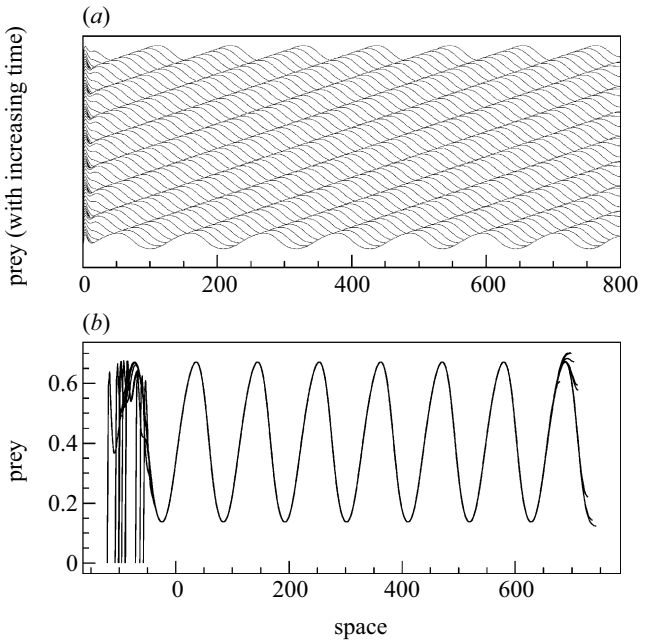

Figure 2. Solutions of the reaction–diffusion model (A 2) in one space dimension. (*a*) A space–time plot, showing periodic travelling waves moving away from the boundary at $x = 0$, that corresponds to the edge of an obstacle. (*b*) The solutions for ten different initial conditions superimposed; the excellent match between the travelling waves generated in the different cases shows that the wave selected is independent of the details of the initial conditions, which is an important indicator of the robustness of our mechanism of periodic-wave generation. In both (*a*) and (*b*), only the prey density is plotted for brevity; the predator density has the same basic form, except for a phase difference in the oscillations. The boundary conditions are zero predator and prey densities at the left-hand boundary ($p = h = 0$ at $x = 0$), corresponding to the edge of an obstacle, and zero flux at the right hand boundary ($\partial p/\partial x = \partial h/\partial x = 0$ at $x = 800$). The dimensionless parameter values are $A = 1.6$, $B = 1.2$, $C = 4.9$, $\delta = 2.5$. In (*a*), the solution is plotted between 5850 and 6000 dimensionless time units, and in (*b*) the plot is after 6000 dimensionless time units; these large times allow transients to dissipate fully. Initially (time $t = 0$), predator and prey densities are chosen randomly, between zero and one, at 60 equally spaced points in the domain, with the values in between determined via linear interpolation. The equations are solved numerically using a semi-implicit Crank–Nicolson method. Note that in (*b*), a small translation is applied to each solution prior to plotting, so that the waves in the different solutions are in phase.

diffusion simulations, the obstacle has little effect when the 'stay put' rule is applied. However, with the 'die' rule, the obstacle significantly alters the spatio-temporal behaviour; the results are best discussed in the context of the behaviour in a homogeneous domain. When there are spatially uniform oscillations in the homogeneous case (such as in figure 3*a*), the obstacle generates periodic travelling waves, moving away from it (figure 3*d*,*g*). When a single spiral wave develops in the homogeneous case (such as in figure 3*b*), the obstacle simply alters this behaviour slightly, with the spiral tending to rotate around the obstacle (figure 3*e*,*h*). Most interesting is the case of parameters for which there are many interacting spirals on a homogeneous domain (such as in figure 3*c*). Obstacle shape then becomes crucial to the results. A square or round obstacle has only a small effect on the spatio-temporal behaviour, that again consists of a number of interacting spirals (figure 3*f*). However, a long, thin obstacle, provided it is sufficiently large, organizes the behaviour into a single spiral wave, rotating around the obstacle (figure 3*i*).

The 'deflect' rule at the obstacle edge gives results that are similar to those of the 'die' rule. Although there are minor differences in behaviour, the key qualitative results are the same with one exception, namely that the tendency of the obstacle to organize interacting spirals into a single spiral is significantly weaker with the 'deflect' rule. Again, with this exception, hybrid rules (such as: 30% of individuals die and 70% deflect) also give very similar results.

4. DISCUSSION

Large-scale landscape features inhibiting dispersal are present in many real ecological systems. We have shown that in the case of a cyclic predator–prey system, such features tend to organize the spatio-temporal dynamics into a coherent pattern, consisting of either a periodic travelling wave or a spiral wave, moving away from the landscape feature. The two cases, periodic wave (also known as target pattern) and spiral wave, are very similar and would be difficult to distinguish without the most detailed spatio-temporal data—even the very detailed Kielder Forest data may not be adequate.

Periodic waves are well known as a solution type in oscillatory systems and have been studied for nearly 30 years (see Kopell & Howard 1973). However, most of this work has focused on the mathematical properties of these waves rather than mechanisms that might cause them to occur in practice. Kaitala & Ranta (1998) have shown that random initial conditions can develop into travelling waves on a small grid of spatial patches; however, this does not generalize to large grids of patches or to a continuous spatial environment. A more general mechanism of periodic-wave generation is invasion—for example, the invasion of a prey population by predators can leave periodic waves in its wake (Sherratt *et al.* 1995, 1997; Petrovskii & Malchow 1999). However, once an invasion is complete, its effects cease and the periodic-wave pattern is vulnerable to alteration by external factors (Kay & Sherratt 1999). In contrast, a large-scale landscape feature can both generate and maintain a pattern of periodic waves as a permanent-solution form over a large area.

The populations in which periodic waves have been studied in most detail are field voles (*M. agrestis*) in the Kielder Forest on the border between Scotland and England and red grouse (*L. lagopus scoticus*) on Kerloch Moor in northeast Scotland. Kielder is one of the largest man-made forests in Europe (613 km^2) and consists mainly of sitka spruce (*Picea sitchensis*) and Norway spruce (*Picea abies*), managed on a 40–60 year rotation. Field voles are common in the grassland areas that follow the cutting of timber and spatio-temporal data on their population dynamics has been gathered since 1984 (Lambin *et al.* 1998; MacKinnon *et al.* 2001). This has shown a pattern of periodic travelling waves, moving in a line about 72° from the north. Notably, this direction is approxi-

mately orthogonal to Kielder Water, a large reservoir (*ca.* 10 km long and 1 km across) in the centre of the forest. Kerloch Moor is dominated by dwarf shrub heather (*Calluna vulgaris*), the main food plant of red grouse. Spatiotemporal data were gathered between 1962 and 1978 (Watson *et al.* 1984; Moss *et al.* 2000) in a part of the moor bounded to the north by farms and woodland (these are not occupied by grouse). The observed travelling wave has a direction approximately perpendicular to this moorland edge.

In both cases, then, the periodic travelling wave moves in a direction that is orthogonal to a large-scale landscape feature. Moreover, the obstacle will rarely be crossed, in both cases. The details of vole behaviour at the edge of Kielder Water are not established, but the size of the reservoir suggests that if the voles attempt to cross it, then the vast majority would fail. Similarly, red grouse are able to cross small areas of farmland, but few would manage to cross the large area that bounds the study region of Watson *et al.* (1984) (Piertney *et al.* 1998). Thus, in both cases, the obstacle edge can reasonably be represented either by the zero population boundary condition that we have considered. Our models then predict travelling waves orthogonal to these obstacles, as found in practice. Of course, both of these real situations have many complexities absent from our model: the presence of other smaller obstacles, strong seasonal effects, etc. Thus more detailed and specific models would be required to fully investigate these two cases.

The causes of the population cycles that are characteristic of many boreal herbivores, including field voles and red grouse, remain unclear. The vole population may cycle due to interaction with common weasels (*Mustela nivalis vulgaris*), a small rodent specialist predator (Turchin & Hanski 1997; Lambin *et al.* 2000); however, there are many other possible causes (Stenseth 1999). In red grouse, recent hypotheses for cyclic behaviour include interaction with a parasite (Hudson *et al.* 1998; see also Lambin *et al.* 1999) and differential territorial behaviour between kin and non-kin (Matthiopoulos *et al.* 1998; MacColl *et al.* 2000). In our modelling, we have focused specifically on cyclic predator–prey systems. However, we believe that the basic phenomenon of periodic waves generated by obstacles is a general feature of oscillatory systems. We have two lines of evidence for this. First, we have found the same behaviour in simulations using other types of oscillatory model, including the Ricker and Lotka–Volterra kinetics. These different models have little in common besides being oscillatory. Second, a more abstract mathematical study using 'normal form' kinetics for oscillatory systems also shows periodic travelling waves generated by obstacles, with the only extension to the behaviour we have reported being that the waves can in some cases travel towards, rather than away from, the obstacle (J. A. Sherratt, in preparation).

Empirical studies of periodic waves depend on the combination of extensive spatio-temporal datasets and new statistical methods (reviewed by Bjørnstad *et al.* 1999). The rarity of such data, coupled with the novelty of the required statistics, mean that it is too early to assess how widespread the phenomenon of travelling waves is in oscillatory populations. But since large-scale landscape features are the rule rather than the exception in real ecological environments, our results suggest that periodic travelling waves are likely to be much more common in the natural world than has previously been assumed.

J.A.S. is supported in part by an Advanced Research Fellowship from Engineering and Physical Sciences Research Council. X.L. was supported in part by a research grant from the National Environment Research Council (NERC). This work was supported in part by NERC and the Scottish Executive Environment and Rural Affairs Department under the Large-Scale Processes in Ecology and Hydrology Thematic Programme (GST/02/1218).

APPENDIX A

Here, we outline the details of the reaction–diffusion model discussed in § 1 and § 2 of the main text. Our model is formulated in terms of predator and prey densities, $p(x, t)$ and $h(x, t)$, where t is time and x denotes position in the one- or two-dimensional domain. We assume that both predator and prey populations disperse via linear diffusion, with dispersal coefficients D_p and D_h respectively; for terrestrial populations, D_p will typically be significantly greater than D_h. Our predator–prey kinetics are standard and have been used previously by a number of authors (for example Nisbet *et al.* (1991) and Dunbar (1986)) and give the following model equations:

$$\text{predators } \frac{\partial p}{\partial t} = \overbrace{D_p\nabla^2 p}^{\text{dispersal}} + \overbrace{akph/1 + kh}^{\substack{\text{benefit from}\\ \text{predation}}} - \overbrace{bp}^{\text{death}} \qquad \text{(A 1}a\text{)}$$

$$\text{prey } \frac{\partial h}{\partial t} = \underbrace{D_h\nabla^2 h}_{\text{dispersal}} + \underbrace{rh(1 - h/h_0)}_{\substack{\text{intrinsic}\\ \text{birth and death}}} - \underbrace{ckph/1 + kh}_{\text{predation}}. \qquad \text{(A 1}b\text{)}$$

Here a, b, c, r, k and h_0 are positive kinetic parameters. The prey consumption rate per predator has a maximal value c at very high prey densities; the constant k reflects how quickly the consumption rate decreases as prey density increases. Parameters a and r denote maximal per capita predator and prey birth rates; for predators, that is the birth rate when the prey density is very high, while for prey it is the birth rate at very low prey density. The per capita predator death rate is denoted by b, and h_0 is the prey carrying capacity.

Equations (A 1) can be simplified somewhat by non-dimensionalizing, using the following rescalings:

$$p^* = p\cdot c/rh_0 \quad h^* = h/h_0 \quad t^* = rt \quad \underline{x}^* = \underline{x}\sqrt{r/D_h}$$

$$\delta^* = D_p/D_h \quad A^* = a/b \quad B^* = r/a \quad C^* = kh_0,$$

where the asterisks denote a dimensionless quantity. Dropping these to ease notation gives the following equations:

$$\frac{\partial p}{\partial t} = \delta\nabla^2 p + \frac{p}{AB}\left[\frac{ACh}{(1 + Ch)} - 1\right] \qquad \text{(A 2}a\text{)}$$

$$\frac{\partial h}{\partial t} = \nabla^2 h + h(1 - h) - \frac{Cph}{(1 + Ch)}. \qquad \text{(A 2}b\text{)}$$

Straightforward mathematical analysis shows that the kinetics in this model are oscillatory provided that the para-

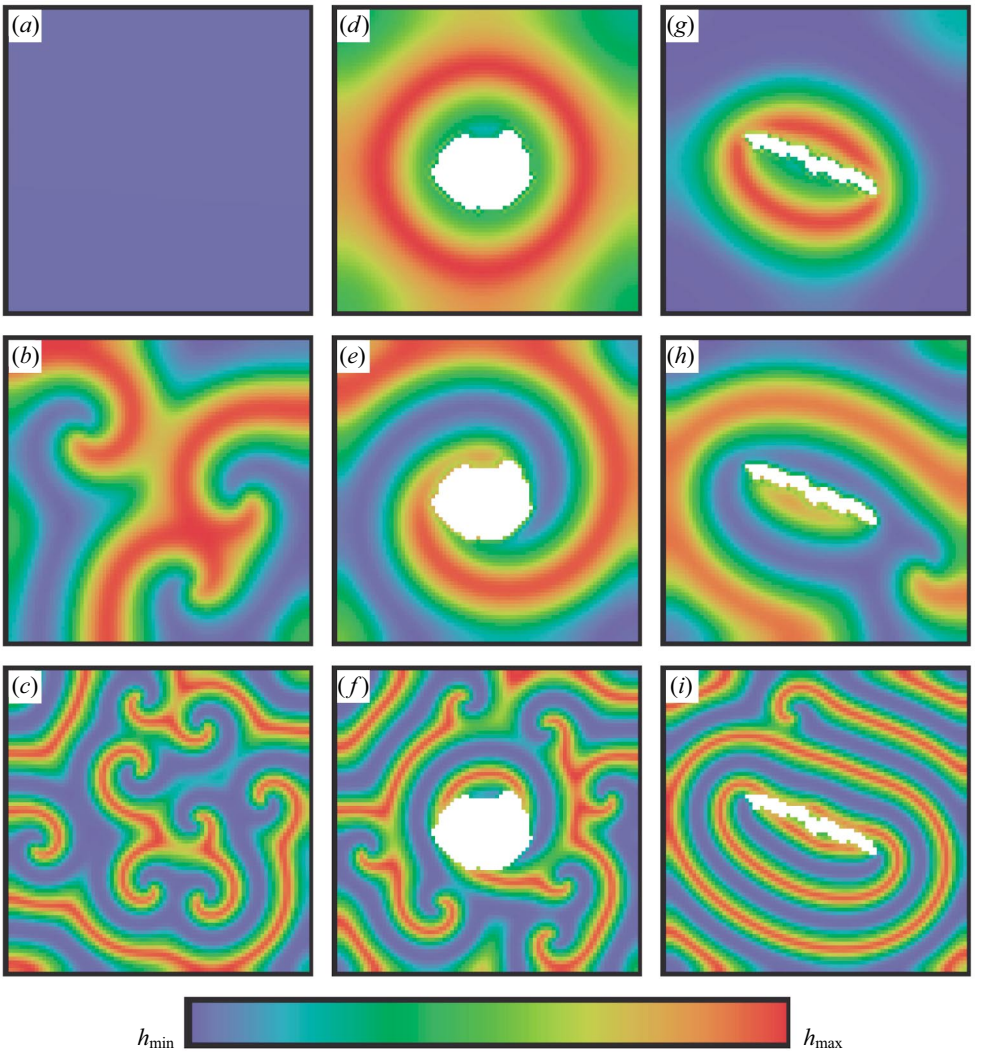

Figure 3. Solutions of the coupled map lattice model, with prey density plotted in space at a single time-point. The rows show simulations for the same set of parameters, with no obstacle (*a–c*), with an approximately circular obstacle (*d–f*) and with a long thin obstacle (*g–i*), using the 'die' rule at the obstacle edge. The columns are for different parameter sets, chosen to give different behaviours in the case of no obstacle. The results show the strong tendency of a landscape feature to generate travelling waves. Note, however, that for the parameters in the third row (*c*,*f*,*i*), travelling waves occur for the long thin obstacle (*i*), but the more irregular dynamics persist when the obstacle is approximately circular (*f*). The model equations (B 1 and B 2) are detailed in Appendix B and the parameter values are: (*a*,*d*,*g*) $a = 2$, $b = 4$, $\nu_h = \nu_p = 0.7$; (*b*,*e*,*h*) $a = 2$, $b = 3.3$, $\nu_h = 0.05$, $\nu_p = 0.4$; (*c*,*f*,*i*) $a = 2$, $b = 4$, $\nu_h = 0.05$, $\nu_p = 0.4$. The limits on the scale bar are chosen differently in each row, for maximum clarity: (*a*,*d*,*g*) and (*c*,*f*,*i*) $h_{min} = 0.16$, $h_{max} = 1.0$; (*b*,*e*,*h*) $h_{min} = 0.33$, $h_{max} = 0.7$. In each case, we solve on an 80 × 80 grid of patches and the solution is plotted after 20 000 time-steps. The initial conditions are generated using a random-number generator before the obstacle is superimposed, with the same seed used for all of the simulations shown. Movie clips corresponding to each part of this figure are available at http://www.ma.hw.ac.uk/~jas/supplements/obstacles/.

meter C is above the critical value $(A + 1)/(A - 1)$; note that $A > 1$ is required for predators and prey to coexist.

In figure 1*a*,*b*, we choose parameter values for this model based on the field vole–weasel interaction; we now summarize briefly the basis for these estimates. The dimensional parameters r and a are the maximal birth rates (when resources are abundant) for prey and predators, respectively. A female field vole (*M. agrestis*) can have as many as six litters per season in optimal conditions, with an average litter size of 5 (Dyczkowski & Yalden 1998). Moreover, early-born females can breed themselves, giving a maximum per capita annual productivity of 27.5 [$= 0.5(6 \times 5 + 2.5 \times 5)$]. Thus $e^r = 27.5 \Rightarrow r = 3.3\ yr^{-1}$. Similarly, when prey is abundant, female weasels (*M. nivalis*) can have two litters per season, averaging six young per litter, and the average of three females in the first litter can breed themselves in the same season (King 1989). This gives a maximum per capita productivity of 15 yr^{-1}, so that $a = 2.7\ yr^{-1}$. Annual mortality for weasels is 77.5% (King 1989), so that $e^{-b} = 0.225 \Rightarrow b = 1.5\ yr^{-1}$. These estimates imply $A \equiv a/b = 1.8$ and $B \equiv r/a = 1.2$. With A and B fixed, we chose C to give an appropriate ratio (about 30) between the maximum and minimum vole densities. In the model, this ratio increases with C and $C = 4.9$ gives the required value. For the vole dispersal coefficient D_h, we assume that 0.05% of individuals move a distance of 2 km in one year; this very rough estimate is based on limited mark-capture data (see Sherratt *et al.* 2000). Neglecting the kinetics and assuming just simple linear diffusion, this implies $D_h \approx 0.2\ km^2\ yr^{-1}$.

The remaining parameter to be estimated is the dispersal coefficient for weasels; this will be larger than that for voles but we are not aware of any relevant data. In figure 1*a*,*b* we arbitrarily assume $\delta = D_h/D_p = 2$; if this ratio is increased, the model continues to predict periodic waves, but of a larger wavelength.

APPENDIX B

In this Appendix, we give details of the coupled map lattice model, that is discussed in § 3. The model assumes a rectangular grid of interconnected patches; most of our simulations are on an 80 patch × 80 patch domain. We solve for the densities of predators p and prey h in each patch, at a series of discrete generations. Following standard modelling procedure, we divide each generation into two substeps: 'dispersal' and 'population kinetics'. In the dispersal substep, a fixed fraction ν_p/ν_h of predators over prey at each patch move to one of the four immediately neighbouring patches; thus

predators

$$p_{i,j}^{t+1/2} = (1 - \nu_p)p_{i,j}^t + \nu_p \frac{p_{i+1,j}^t + p_{i-1,j}^t + p_{i,j+1}^t + p_{i,j-1}^t}{4} \quad \text{(B 1}a\text{)}$$

prey

$$h_{i,j}^{t+1/2} = (1 - \nu_h)h_{i,j}^t + \nu_h \frac{h_{i+1,j}^t + h_{i-1,j}^t + h_{i,j+1}^t + h_{i,j-1}^t}{4}. \quad \text{(B 1}b\text{)}$$

Here (i,j) denotes patch location within our grid of patches, and the integer t denotes the time-step. The parameters ν_h and ν_p give a measure of population dispersal: a value of 0.05 would correspond to a relatively low movement rate, while 0.2 or more would indicate a rapidly dispersing population (Sherratt *et al.* 2000).

In the population kinetics substep, the populations in each patch change independently. The kinetics thus have the form of coupled difference equations for predator and prey densities, which apply at each patch. There are many such models in the literature (see May (1981) or Murray (1989) for reviews) and we use the model initially proposed by Beddington *et al.* (1975). By suitably rescaling the population densities, this model can be written as

$$\text{predators } p_{i,j}^{t+1} = h_{i,j}^{t+1/2}[1 - \exp(-bp_{i,j}^{t+1/2})] \quad \text{(B 2}a\text{)}$$

$$\text{prey } h_{i,j}^{t+1} = h_{i,j}^{t+1/2} \exp[a(1 - h_{i,j}^{t+1/2}) - bp_{i,j}^{t+1/2}]. \quad \text{(B 2}b\text{)}$$

These equations imply a unique coexistence steady state if $b > 1$, which is unstable provided a and b are not too small. For a range of parameter values, the kinetics then have the form of periodic or quasi-periodic cycles in the two populations and we have solved the model only in this region of parameter space. When a is large with b close to 1, very different and much more irregular kinetics occur, but such cases are not relevant to our study, that is concerned specifically with cyclic populations.

REFERENCES

Beddington, J. R., Free, C. A. & Lawton, J. H. 1975 Dynamic complexity in predator–prey models framed in difference equations. *Nature* **255**, 58–60.

Bjørnstad, O. N., Ims, R. A. & Lambin, X. 1999 Spatial population dynamics analyzing patterns and processes of population synchrony. *Trends Ecol. Evol.* **14**, 427–432.

Dunbar, S. R. 1986 Travelling waves in diffusive predator–prey equations—periodic orbits and point-to-periodic heteroclinic connections. *Soc. Ind. Appl. Math. J. Appl. Math.* **46**, 1057–1078.

Dyczkowski, J. & Yalden, D. W. 1998 An estimate of the impact of predators on the British field vole *Microtus agrestis* population. *Mammal Rev.* **28**, 165–184.

Hassell, M. P., Comins, H. N. & May, R. M. 1991 Spatial structure and chaos in insect population dynamics. *Nature* **353**, 255–258.

Hudson, P. J., Dobson, A. P. & Newborn, D. 1998 Prevention of population cycles by parasite removal. *Science* **282**, 2256–2258.

Kaitala, V. & Ranta, E. 1998 Travellling wave dynamics and self-organisation in a spatio-temporally structured population. *Ecol. Lett.* **1**, 186–192.

Kay, A. L. & Sherratt, J. A. 1999 On the persistence of spatio-temporal oscillations generated by invasion. *IMA J. Appl. Math.* **63**, 199–216.

King, C. 1989 *The natural history of weasels and stoats*. London: Croom Helm.

Kopell, N. & Howard, L. N. 1973 Plane wave solutions to reaction–diffusion equations. *Stud. Appl. Math.* **52**, 291–328.

Lambin, X., Elston, D. A., Petty, S. J. & MacKinnon, J. L. 1998 Spatial asynchrony and periodic travelling waves in cyclic populations of field voles. *Proc. R. Soc. Lond.* B **265**, 1491–1496.

Lambin, X., Krebs, C. J., Moss, R., Stenseth, N. C. & Yoccoz, N. G. 1999 Population cycles and parasitism. *Science* **286**, 2425.

Lambin, X., Petty, S. J. & MacKinnon, J. L. 2000 Cyclic dynamics in field vole populations and generalist predation. *J. Anim. Ecol.* **69**, 106–118.

MacColl, A. D. C., Piertney, S. B., Moss, R. & Lambin, X. 2000 Spatial arrangement of kin affects recruitment success in young male red grouse. *Oikos* **90**, 261–270.

MacKinnon, J. L., Lambin, X., Elston, D. A., Thomas, C. J., Sherratt, T. N. & Petty, S. J. 2001 Scale invariant spatio-temporal patterns of field vole density. *J. Anim. Ecol.* **70**, 101–111.

Matthiopoulos, J., Moss, R. & Lambin, X. 1998 Models of red grouse cycles. A family affair? *Oikos* **82**, 574–590.

May, R. M. 1981 *Stability and complexity in model ecosystems*. Princeton University Press.

Moss, R., Elston, D. A. & Watson, A. 2000 Spatial asynchrony and demographic travelling waves during red grouse population cycles. *Ecology* **81**, 981–989.

Murray, J. D. 1989 *Mathematical biology*. Berlin: Springer.

Nisbet, R. M., McCauley, E., De Roos, A. M., Murdoch, W. W. & Gurney, W. S. C. 1991 Population dynamics and element recycling in an aquatic plant herbivore system. *Theor. Pop. Biol.* **40**, 125–147.

Petrovskii, S. V. & Malchow, H. 1999 A minimal model of pattern formation in a prey predator system. *Math. Comput. Modelling* **29**, 49–63.

Piertney, S. B., MacColl, A. D. C., Bacon, P. J. & Dallas, J. F. 1998 Local genetic structure in red grouse (*Lagopus lagopus scoticus*): evidence from microsatellite DNA markers. *Mol. Ecol.* **7**, 1645–1654.

Sherratt, J. A. 2002 Dirichlet boundary conditions generate periodic travelling waves in oscillatory reaction diffusion systems. (In preparation.).

Sherratt, J. A., Lewis, M. A. & Fowler, A. C. 1995 Ecological chaos in the wake of invasion. *Proc. Natl Acad. Sci. USA* **92**, 2524–2528.

Sherratt, J. A., Eagan, B. T. & Lewis, M. A. 1997 Oscillations and chaos behind predator–prey invasion: mathematical artefact or ecological reality? *Phil. Trans. R. Soc* B **352**, 21–38.

Sherratt, T. N., Lambin, X., Petty, S. J., MacKinnon, J. L., Coles, C. F. & Thomas, C. J. 2000 Application of coupled oscillator models to understand extensive synchrony domains and travelling waves in populations of the field vole in Kielder forest, UK. *J. Appl. Ecol.* **37**, 148–158.

Stenseth, N. C. 1999 Population cycles in voles and lemmings: density dependence and phase dependence in a stochastic world. *Oikos* **87**, 427–461.

Turchin, P. & Hanski, I. 1997 An empirically based model for latitudinal gradient in vole population dynamics. *Am. Nat.* **149**, 842–874.

Watson, A., Moss, R., Rothery, P. & Parr, R. 1984 Demographic causes and predictive models of population fluctuations in Red Grouse. *J. Anim. Ecol.* **54**, 639–662.

As this paper exceeds the maximum length normally permitted, the authors have agreed to contribute to production costs.